Supporting Information

Self-Assembled Molecular Rafts at Liquid|Liquid Interfaces for Four-Electron Oxygen Reduction

*Astrid J. Olaya[a], Delphine Schaming[a], Pierre-Francois Brevet[b], Hirohisa Nagatani[c], Tomas Zimmermann[d], Jiri Vanicek[d], Hai-Jun Xu[e], Claude P. Gros[e], Jean-Michel Barbe[e] and Hubert H. Girault[a]***

[a]Laboratoire d'Electrochimie Physique et Analytique, Station 6, Ecole Polytechnique Fédérale de Lausanne, CH-1015 Lausanne, Switzerland.

[b]Laboratoire de Spectrométrie Ionique et Moléculaire, UMR CNRS 5579, Université Claude Bernard Lyon 1, 43 Bd du 11 Novembre 1918, 69622 Villeurbanne cedex, France.

[c]Faculty of Chemistry, Institute of Science and Engineering, Kanazawa University, Kakuma, Kanazawa 920-1192, Japan.

[d]Laboratory of Theoretical Physical Chemistry, Institut des Sciences et Ingénierie Chimiques, Ecole Polytechnique Fédérale de Lausanne, CH-1015 Lausanne, Switzerland.

[e]Institut de Chimie Moléculaire de l'Université de Bourgogne, ICMUB (UMR 5260, CNRS), France.

Contents

Complete reference 30:

Frisch, M. J.; Trucks, G. W. T.; Schlegel, H. B.; Scuseria, G. E.; Robb, M. A.; Cheeseman, J. R.; Scalmani, G.; Barone, V.; Mennucci, B.; Petersson, G. A.; Nakatsuji, H.; Caricato, M.; Li, X.; Hratchian, H. P.; Izmaylov, A. F.; Bloino, J.; Zheng, G.; Sonnenberg, J. L.; Hada, M.; Ehara, M.; Toyota, K.; Fukuda, R.; Hasegawa, J.; Ishida, M.; Nakajima, T.; Honda, Y.; Kitao, O.; Nakai, H.; Vreven, T.; Montgomery, Jr., J. A.; Peralta, J. E.; Ogliaro, F.; Bearpark, M.; Heyd, J. J.; Brothers, E.; Kudin, K. N.; Staroverov, V. N.; Kobayashi, R.; Normand, J.; Raghavachari, K.; Rendell, A.; Burant, J. C.; Iyengar, S. S.; Tomasi, J.; Cossi, M.; Rega, N.; Millam, J. M.; Klene, M.; Knox, J. E.; Cross, J. B.; Bakken, V.; Adamo, C.; Jaramillo, J.; Gomperts, R.; Stratmann, R. E.; Yazyev, O.; Austin, A. J.; Cammi, R.; Pomelli, C.; Ochterski, J. W.; Martin, R. L.; Morokuma, K.; Zakrzewski, V. G.; Voth, G. A.; Salvador, P.; Dannenberg, J. J.; Dapprich, S.; Daniels, A. D.; Farkas, Ö.; Foresman, J. B.; Ortiz, J. V.; Cioslowski, J.; Fox, D. J. Gaussian 09, Revision A.01: Gaussian Inc.: Wallingford CT, **2009**

SI1. Surface Second Harmonic Generation [1]

The intensity of the SSHG response (I (2ω)) can be expressed in terms of the nonlinear polarization (P(2ω)) induced by the fundamental driving field at frequency ω (Eq. S1).

$$I_{SSHG}(2\omega) \propto \left[P(2\omega)\right]^2 \qquad \text{S1}$$

The nonlinear polarization is directly proportional to the macroscopic second order nonlinear susceptibility tensor ($\chi^{(2)}$), and to the intensity of the driving field at frequency ω (E_L(ω)) as shown in Eq. S2.

$$P(2\omega) \propto \overleftrightarrow{\chi}^{(2)} : E_L(\omega)E_L(\omega) \qquad \text{S2}$$

As shown in Eq. S3, the macroscopic susceptibility tensor $\chi^{(2)}$ and therefore I (2ω), are directly proportional to the surface density of the adsorbed molecules at the interface (N_s) and the molecular hyperpolarizability ($\langle\beta\rangle$)

$$\overleftrightarrow{\chi}^{(2)} = \frac{1}{\varepsilon_0}\sum_i N_{s,i}\left\langle\overleftrightarrow{T}_i\right\rangle\overrightarrow{\beta}_i \qquad \text{S3}$$

where, T_i is the transformation tensor for each molecule of type i (necessary for the transformation from the molecular reference frame) and ε_0 is the permittivity in the vacuum.

When no analyzer is used at the outlet of the cell, the outlet polarization is a combination of both contributions p and s (Eq. S4). Such contributions are expressed in Eq. S5 and S6 as a function of the incident beam angle γ.

$$I_{SSHG}(2\omega) = I^{p-out} + I^{s-out} \qquad \text{S4}$$

$$I_{SSHG}^{p-out}(2\omega) = K\left[a\cos^2\gamma + b\sin^2\gamma\right]^2 \qquad \text{S5}$$

$$I_{SSHG}^{s-out}(2\omega) = K\left[c\sin^2\gamma\right]^2 \qquad \text{S6}$$

SI2. Synthesis and characterization of the porphyrins

Synthesis of 5,10,15,20-tetra-(4-N-methylpyridyl)-porphyrin tetraiodide Cobalt(II) CoTMPyP^{4+} (1)

5,10,15,20-Tetrapyridylporphyrin [2,3] (0.50 g, 0.808 mmol) and $Co(OAc)_2 \cdot 4H_2O$ (0.50 g, 2 mmol) were dissolved in DMF (50 mL) under Ar. The reaction mixture was heated to reflux for 3.5 hours in the dark (see Figure S7). The reaction was monitored by MALDI/TOF mass spectrometry. CH_3I (5 mL) was then added dropwise under Ar and the reaction mixture was refluxed for another 6.5 hours. After cooling the reaction mixture to room temperature, the organic solvent was removed under reduced pressure. The product was purified by recrystallization from H_2O/acetone. Yield: 880 mg, 87%. UV/Vis (2%DMF-CH_3OH): l_{max} (nm) (e x 10^{-3} L mol^{-1} cm^{-1}) = 430.0 (84.1), 535.9 (8.6). The spectroscopic data are in agreement with the literature [4].

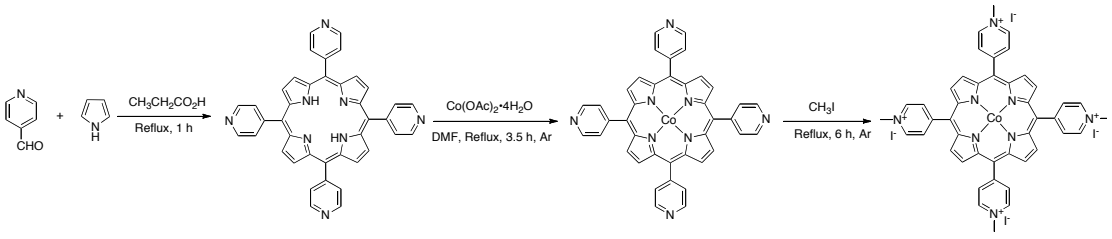

Figure SI1. Schematic representation of the synthetic route of CoTMPyP^{4+}.

Synthesis of tetrasodium 5,10,15,20-tetra(4-sulfophenyl)porphyrin Cobalt(II) CoTPPS^{4-} (2)

Tetrasodium tetra(4-sulfophenyl)porphyrin [5] (TPPS) (400 mg, 0.391 mmol) was dissolved in 95:5 methanol/ water (40 mL) under Argon. $Co(OAc)_2 \cdot 4H_2O$ (249 mg, 1 mmol) was added to the porphyrin solution (see Fig. S8). The mixture was heated to reflux. The reaction was followed by UV-Visible spectroscopy. After refluxing overnight, the reaction mixture was cooled to room temperature. Cobalt

complex was precipitated by adding acetone slowly and filtered. The filtrate was washed with acetone. The pure product was obtained by recrystallization from CH_3OH/acetone. Yield: 274 mg, 65%. ESI-MS: m/z 336.65 $[M\text{-}3Na^+]^{3-}$. UV/Vis (CH_3OH): l_{max} (nm) (e x 10^{-3} L mol^{-1} cm^{-1}) = 412.9 (199.6), 529.0 (13.5). The spectroscopic data are in agreement with the literature [6].

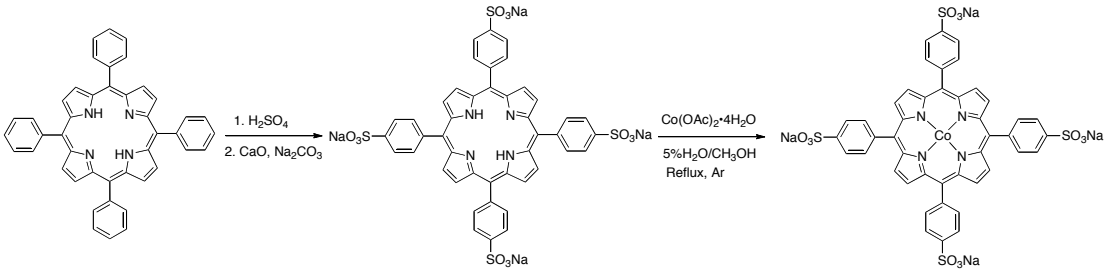

Figure SI2. Schematic representation of the synthetic route of **CoTPPS^{4-}**.

Synthesis of the cofacial porphyrins: Co_2(DPX), Co_2(DPO), and Co_2(DPOx)

Details on the synthesis and characterization of each cofacial porphyrin [Co_2(DPX), Co_2(DPO), and Co_2(DPOx)] have been reported elsewhere [7-11] (see Figure S9).

Co_2(DPX): The porphyrin free-base H_4(DPX) (70 mg, 60 μmol) was dissolved in distilled and degassed CH_2Cl_2 (15 mL) under an argon atmosphere and a degassed MeOH solution (5 mL) containing cobalt(II) acetate tetrahydrate (75 mg, 0.3 mmol) was added. The reaction mixture was refluxed for one hour (the reaction was monitored by MALDI/TOF mass spectrometry and UV/Vis spectroscopy), and then cooled to room temperature and the solvent was evaporated using the Schlenk line. The product was purified under argon by column chromatography (Al_2O_3, eluent: CH_2Cl_2) affording after evaporation of the solvent under vacuum the biscobalt bisporphyrin **Co_2(DPX)** as a purple solid (52 mg, 41 μmol, 67%). MS (MALDI/TOF) *m/z* = 1276.4 $[M]^{+\cdot}$, 1276.5 calcd. for

$C_{79}H_{82}Co_2N_8O$. UV/Vis (CH_2Cl_2): l_{max} (nm) ($\varepsilon \times 10^{-3}$ in $L.mol^{-1}.cm^{-1}$) = 385 (185); 524 (9.8); 559 (12.4). The spectroscopic data are in agreement with the literature [7-11].

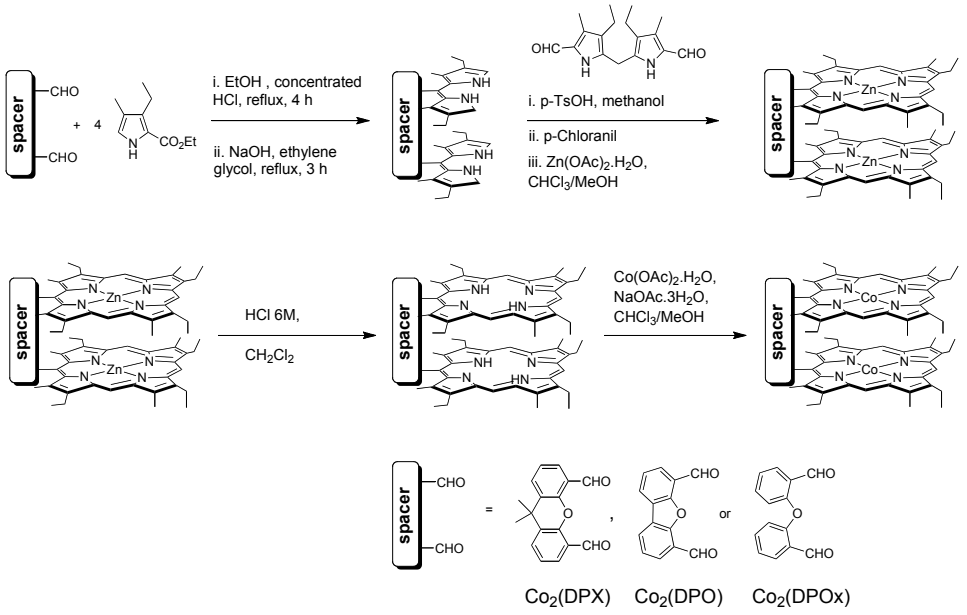

Figure SI3. Schematic representation of the synthetic route of Co_2(DPOx), Co_2(DPX), and Co_2(DPO).

Co_2(DPO) was synthesized as described for **Co_2(DPX)** under an inert atmosphere from 100 mg (92 µmol) of the corresponding free-base dyad H_4(DPO) and 125 mg (0.5 mmol) of cobalt acetate tetrahydrate in 20 mL of a refluxing MeOH/CH_2Cl_2 (1:4) mixture. After purification, the title bis-Co dyad was obtained in 72% yield (79 mg, 64 µmol). MS (MALDI/TOF): *m/z* 1234.4 $[M]^{+\cdot}$, 1234.4 calcd. for $C_{76}H_{76}Co_2N_8O$. UV/Vis (CH_2Cl_2): λ_{max}, nm ($\varepsilon \times 10^{-3}$ in $M^{-1}.cm^{-1}$) 392 (212); 526 (10.2); 555 (16.1). The spectroscopic data are in agreement with the literature [7-11].

Co_2(DPOx) was synthesized as described for **Co_2(DPX)** under an inert atmosphere from 100 mg (89 µmol) of the corresponding free-base dyad H_4(DPOx) and 125 mg (0.5 mmol) of cobalt acetate tetrahydrate in 20 mL of a refluxing MeOH/CH_2Cl_2 (1:4) mixture. After purification, the title bis-Co

dyad was obtained in 68% yield (75 mg, 60 μmol). MS (MALDI/TOF): *m/z* 1236.5 $[M]^{+\cdot}$, 1236.5 calcd. for $C_{76}H_{78}N_8OCo_2$. UV/Vis (CH_2Cl_2): λ_{max}, nm ($\varepsilon \times 10^{-3}$ in $M^{-1}.cm^{-1}$) 388 (165); 524 (9.8); 558 (16.4). The spectroscopic data are in agreement with the literature [7-11].

Physicochemical Characterization of the porphyrins

^1H NMR spectra for synthesized compounds were recorded on a Bruker DRX–300 AVANCE spectrometer. Chemical shifts for ^1H NMR spectra are expressed in parts per million (ppm) relative to $CDCl_3$ (7.28 ppm) and DMSO-D_6 (2.52 ppm). The mass spectra were obtained on a Bruker Daltonics Ultraflex II spectrometer at the *Université de Bourgogne* in the MALDI/TOF reflectron mode using dithranol as a matrix. High resolution mass measurements (HR–MS) were carried on a Bruker Micro–ToF Q instrument in ESI mode. UV/Vis spectra were recorded on a Varian Cary 1 spectrophotometer.

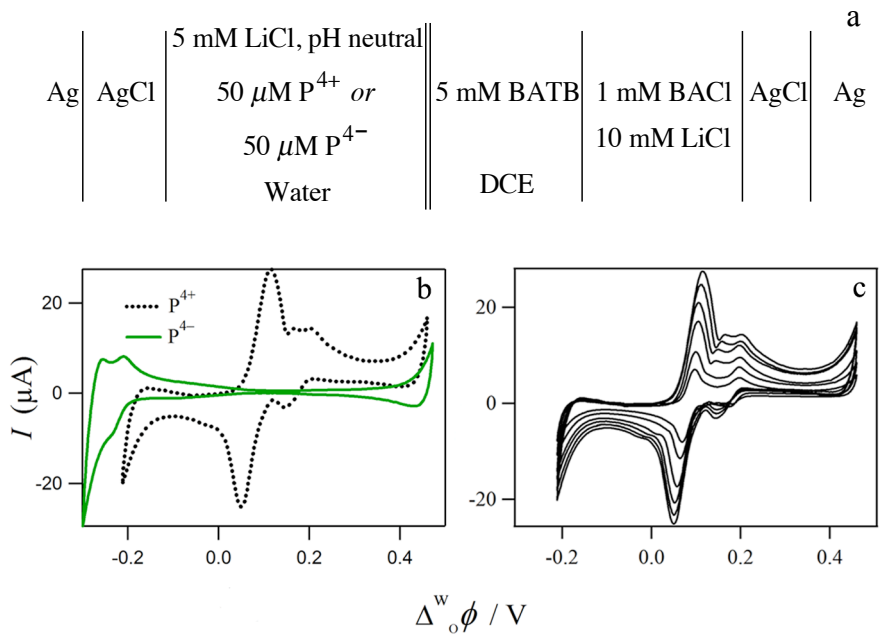

Figure SI4. Ion-transfer voltammetry. (a) Initial electrochemical cell composition of the four-electrode cell used to study the transfer of the porphyrins. P^{4+}:CoTMPyP^{4+}, P^{4-}: CoTPPS^{4-}; (b) Ion-transfer voltammogram of 50 μM CoTMPyP^{4+} (P^{4+}) and 50 μM CoTPPS^{4-} (P^{4-}) at neutral pH and 50 mV• s^{-1}. (c) Scan rate dependence of the ion transfer of P^{4+} at neutral pH. The voltammetric responses associated with the transfer from the aqueous to the organic phase of the cationic porphyrin shows three peaks in the middle of the potential window. The most intense signal is associated with the transfer of the porphyrin, with a half-wave transfer potential ($\Delta_o^w\phi_{1/2,}$) of 0.08 V, while the post peaks around 0.15 V and 0.20 V that increases linearly with the scan rate, are related to strong adsorption of the porphyrin at the aqueous side of the liquid/liquid junction. The transfer of P^{4-} is located at the limit of the potential window close to the transfer of Cl^- with a $\Delta_o^w\phi_{1/2,}$ around –0.22 V. No adsorption peaks are observed for this porphyrin.

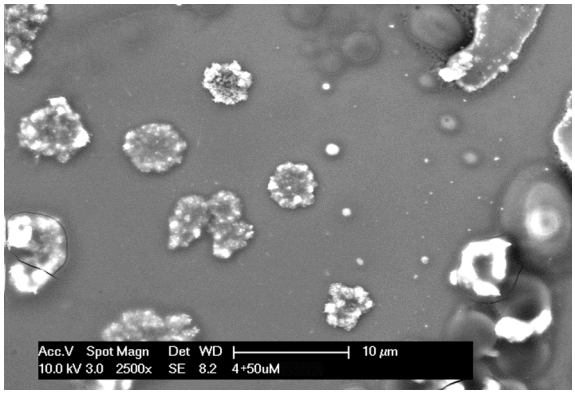

Figure SI5. Secondary electrons SEM picture of P^{4+} cristalized directly from water.

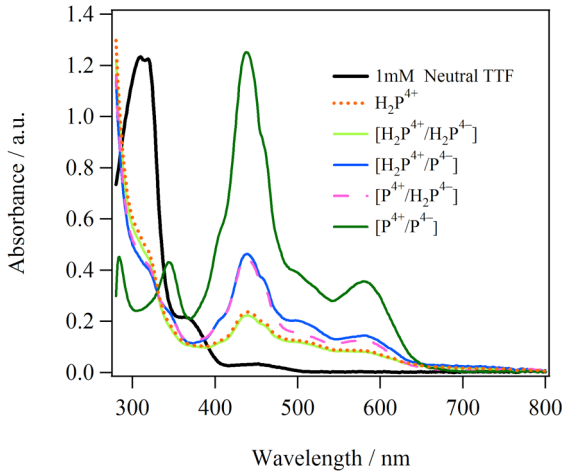

Figure SI6. UV-visible absorption spectra of the organic phase after 1 h of biphasic reaction by using the cell illustrated in Figure 2a. P^{4+} :CoTMPyP^{4+}, P^{4-}: CoTPPS^{4-}, [P^{4+}/P^{4-}]: Equimolar mixture of both porphyrins. H_2P^{4+}: H_2TMPyP^{4+}, H_2P^{4-}: H_2TPPS^{4-}. The concentration of the porphyrins was 50 µM.

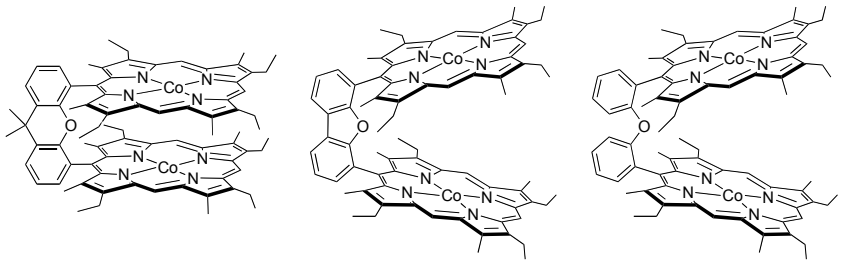

Figure SI7. Chemical structures of the cofacial porphyrins Co_2(DPX), Co_2(DPO) and Co_2(DPOx).

References

(1) Brevet, P. F. *Second Harmonic Generation*; Presses polytechniques et universitaires romandes: Lausanne, 1997.

(2) Tovmasyan, A. G.; Babayan, N. S.; Sahakyan, L. A.; Shahkhatuni, A. G.; Gasparyan, G. H.; Aroutiounian, R. M.; Ghazaryan, R. K. *J. Porphyr. Phthalocya.* **2008**, *12*, 1100-1110.

(3) Adler, A. D.; Longo, F. R.; Finarelli, J. D.; Goldmacher, J.; Assour, J.; Korsakoff, L. *J. Org. Chem.* **1967**, *32*, 476-476.

(4) Li, J.; Wei, Y.; Guo, L.; Zhang, C.; Jiao, Y.; Shuang, S.; Dong, C. *Talanta* **2008**, *76*, 34-39.

(5) Srivastava, T. S.; Tsutsui, M. *J. Org. Chem.* **1973**, *38*, 2103-2103.

(6) Molaei Rad, A.; Akbar Moosavi-Movahedi, A.; Ghourchian, H.; Safari, N.; Hong, J.; Moosavi-Movahedi, Z.; Nazari, K.; Akbar Saboury, A.; Rajabali Jamaat, P. *J. Porphyr. Phthalocya.* **2007**, *11*, 836-845.

(7) Chang, C. J.; Deng, Y.; Heyduk, A. F.; Chang, C. K.; Nocera, D. G. *Inorg. Chem.* **2000**, *39*, 959-966.

(8) Chang, C. J.; Deng, Y.; Shi, C.; Chang, C. K.; Anson, F. C.; Nocera, D. G. *Chem. Commun.* **2000**, 1355-1356.

(9) Deng, Y.; Chang, C. J.; Nocera, D. G. *J. Am. Chem. Soc.* **2000**, *122*, 410-411.

(10) Fukuzumi, S.; Okamoto, K.; Gros, C. P.; Guilard, R. *J. Am. Chem. Soc.* **2004**, *126*, 10441-10449.

(11) Chen, P.; Lau, H.; Habermeyer, B.; Gros, C. P.; Barbe, J. M.; Kadish, K. M. *J. Porphyr. Phthalocya.* **2011**, *15*, 467-479.